ACS central science

Research Article

http://pubs.acs.org/journal/acscii

Catalytic Oxidation of Methane into Methanol over Copper-Exchanged Zeolites with Oxygen at Low Temperature

Karthik Narsimhan, Kenta Iyoki, Kimberly Dinh, and Yuriy Román-Leshkov*

Department of Chemical Engineering, Massachusetts Institute of Technology, 77 Massachusetts Avenue, Cambridge, Massachusetts 02139, United States

Supporting Information

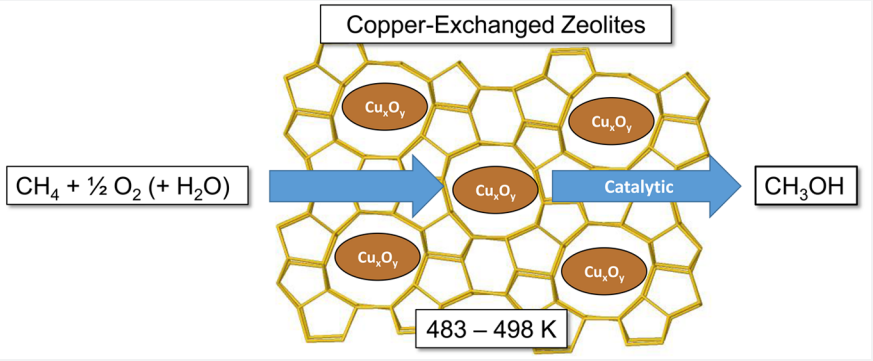

ABSTRACT: The direct catalytic conversion of methane to liquid oxygenated compounds, such as methanol or dimethyl ether, at low temperature using molecular oxygen is a grand challenge in C−H activation that has never been met with synthetic, heterogeneous catalysts. We report the first demonstration of direct, catalytic oxidation of methane into methanol with molecular oxygen over copper-exchanged zeolites at low reaction temperatures (483−498 K). Reaction kinetics studies show sustained catalytic activity and high selectivity for a variety of commercially available zeolite topologies under mild conditions (e.g., 483 K and atmospheric pressure). Transient and steady state measurements with isotopically labeled molecules confirm catalytic turnover. The catalytic rates and apparent activation energies are affected by the zeolite topology, with caged-based zeolites (e.g., Cu-SSZ-13) showing the highest rates. Although the reaction rates are low, the discovery of catalytic sites in copper-exchanged zeolites will accelerate the development of strategies to directly oxidize methane into methanol under mild conditions.

To date, no man-made catalyst can convert methane (CH_4) and oxygen (O_2) directly into methanol (CH_3OH) at low temperature. For more than 100 years, the selective oxidation of this simple alkane has remained unsolved. This transformation, however, is essential to exploit our highly abundant natural gas reserves, particularly those located in distributed fields or stranded wells that cannot be accessed with large, capital-intensive reforming facilities. Although oxidative C−H bond activation of CH_4 is thermodynamically and kinetically accessible at low temperatures, the large bond dissociation energy (435 kJ mol^{-1}) of this molecule hinders C−H cleavage reactions via homolytic or heterolytic pathways. Consequently, few catalysts are capable of preventing overoxidation to carbon dioxide (CO_2). Several alternative strategies for activating methane have been reported, including multistep oxyfunctionalization with Periana catalysts,[1,2] borylation,[3] and electrophilic carbene insertion,[4,5] but all have fallen short of producing methanol directly and do not use oxygen as the oxidizing agent. In contrast, methane monooxygenase enzymes are capable of oxidizing CH_4 selectively into CH_3OH using O_2 at room temperature.[6−8] While such biocatalysts are difficult to scale-up, the nature of their active sites provides inspiration for the development of synthetic oxidation catalysts. In this respect, iron-[9,10] and copper-[11−13] exchanged zeolites have emerged as a promising class of materials capable of selectively oxidizing CH_4 into surface-bound methoxy species by hosting active sites akin to those found in CH_4 monooxygenases. Despite their potential, these materials have only been shown to oxidize CH_4 to CH_3OH stepwise and stoichiometrically with molecular oxygen (O_2)[11,14,15] or catalytically with hydrogen peroxide,[16] making the process prohibitively expensive. Here, we report the first instance of catalytic gas phase oxidation of CH_4 into CH_3OH with O_2 under mild conditions. Copper-exchanged zeolite catalysts of various topologies maintain sustained activity and high CH_3OH selectivity at 483 K, while transient kinetic experiments with isotopically labeled molecules confirm catalytic turnover. The discovery of catalytically active sites for CH_3OH production in zeolites will be the foundation to develop new strategies for low temperature catalytic methane oxidation.

The stoichiometric oxidation of CH_4 to CH_3OH over copper-exchanged zeolites is believed to occur over mono-(μ-

Received: May 9, 2016
Published: June 13, 2016

DOI: 10.1021/acscentsci.6b00139
ACS Cent. Sci. 2016, 2, 424−429

oxo) dicupric cores[13,17] or $[Cu_3O_3]^{2+}$ trimeric sites[18,19] generated by flowing anhydrous O_2 over the zeolite at temperatures above 723 K. These highly reactive electrophilic metal−oxygen species are adept at attacking the strong C−H bonds of CH_4, generating surface-bound methoxy groups at temperatures below 473 K.[12] Methoxy groups are typically extracted as CH_3OH by reacting with H_2O, which deactivates the copper sites and necessitates high temperature reactivation under anhydrous O_2 to perform the next oxidation cycle.[13,15] In the present study, stoichiometric and catalytic CH_3OH production regimes are observed during the gas phase oxidation of CH_4 over copper-exchanged zeolites with the MFI topology in the sodium (Cu-Na-ZSM-5) or proton (Cu-H-ZSM-5) forms at 483 K and atmospheric pressure (Figure 1). Similar to

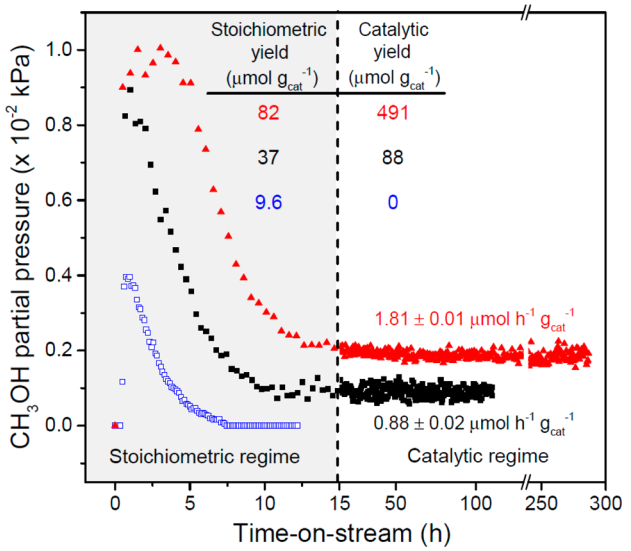

Figure 1. CH_4 oxidation over Cu-ZSM-5. Catalyst pretreatment: 5 h at 823 K under flowing O_2, cooled to 483 K under O_2 flow and then purged under He for 0.5 h. Initial dry CH_4 oxidation: 0.5 h under 2400 mL h^{-1} g$_{cat}^{-1}$ of CH_4 at 483 K. CH_3OH partial pressure (kPa) with $He/H_2O/O_2$ over (blue open squares) Cu-Na-ZSM-5 (Cu/Al = 0.37, Na/Al = 0.26): T = 483 K, WHSV = 2400 mL h^{-1} g$_{cat}^{-1}$, P_{He} = 98.1 kPa, P_{H_2O} = 3.2 kPa, P_{O_2} = 0.0025 kPa (25 ppm). CH_3OH partial pressure (kPa) with CH_4, H_2O, and O_2 over (■) Cu-Na-ZSM-5 and (red solid triangles) Cu-H-ZSM-5 (Cu/Al = 0.31): T = 483 K, WHSV = 2400 mL h^{-1} g$_{cat}^{-1}$, P_{CH_4} = 98.1 kPa, P_{H_2O} = 3.2 kPa, P_{O_2} = 0.0025 kPa (25 ppm).

previous studies, the catalysts were activated under flowing O_2 at 823 K, cooled to reaction temperature, purged with helium (He) for 1 h, and contacted with a pure CH_4 stream for 0.5 h.[11,13,14] However, unlike previous studies using only H_2O for extraction, we hydrolyzed surface-bound methoxy species by flowing a gas mixture comprised of 3.2 kPa of H_2O, 0.0025 kPa of O_2 and balance CH_4. Under these conditions, Cu-Na-ZSM-5 (Cu/Al = 0.37, Na/Al = 0.26) and Cu-H-ZSM-5 (Cu/Al = 0.31) evolved 37 μmol g$_{cat}^{-1}$ and 82 μmol g$_{cat}^{-1}$ of stoichiometric CH_3OH, respectively. These values are more than two times higher than those obtained with Cu-Na-ZSM-5 using only He, O_2, and H_2O as the extracting gas (9.6 μmol g$_{cat}^{-1}$) or those reported by Lobo et al. (16 μmol g$_{cat}^{-1}$)[20] using 3.2 kPa H_2O in N_2 at 473 K and Schoonheydt et al. (8 μmol g$_{cat}^{-1}$)[11,14] using a 50% v/v acetonitrile aqueous solution for 1 h at 298 K to extract the oxidized products.

Remarkably, sustained CH_4 oxidation activity was observed when continuing to feed the CH_4, H_2O, and O_2 gas mixture after all stoichiometric CH_3OH was extracted (Figure 1). Steady state CH_3OH production rates of 0.88 ± 0.02 μmol h^{-1} g$_{cat}^{-1}$ and 1.81 ± 0.01 μmol h^{-1} g$_{cat}^{-1}$ were measured for Cu-Na-ZSM-5 and Cu-H-ZSM-5, respectively. Over Cu-Na-ZSM-5, CH_3OH was the main product generated (as determined by ^{1}H nuclear magnetic resonance, Figure S1) with a selectivity of 70.6 ± 0.4%, while CO_2 was the only byproduct generated at a rate of 0.38 ± 0.02 μmol h^{-1} g$_{cat}^{-1}$ (Figure S2). CO_2 selectivity did not increase when higher conversions were simulated by introducing CH_3OH as a reagent at identical conditions (Supporting Information, Section S2, Figures S3−S4), although most of CH_3OH was dehydrated into dimethyl ether in the presence of acid sites at these conditions (>60% yield). Notably, the steady state CH_3OH production rates persisted without apparent deactivation, generating a total of 88 μmol g$_{cat}^{-1}$ over 108 h with Cu-Na-ZSM-5—a value roughly five times higher than that reported for the stoichiometric oxidation over Cu-Na-ZSM-5.[20] Similarly, Cu-H-ZSM-5 generated a total of 491 μmol g$_{cat}^{-1}$ over 288 h—a value ca. 1.4 times larger than the total copper content of the zeolite (Figure S5). The excess CH_3OH produced per copper atom in Cu-H-ZSM-5 coupled with the lack of sustained CH_3OH production in the absence of CH_4 in the extracting gas mixture over Cu-Na-ZSM-5 (Figure 1, open symbols) are strong evidence that CH_4 is oxidized catalytically over H_2O-tolerant copper sites.

Catalytic turnover was verified with transient experiments using isotopically labeled molecules coupled with online mass spectrometry (MS). ^{13}C methoxy species were deposited on the zeolite by flowing $^{13}CH_4$ (16.8 kPa $^{13}CH_4$ [99 atom % ^{13}C, Sigma-Aldrich] with balance He) over an activated Cu-Na-ZSM-5 sample for 0.5 h at 483 K and then flowing a regular $^{12}CH_4/H_2O/O_2$ gas mixture to extract the methoxy species (detailed procedure found in Figure S6A). As shown in Figure 2, enriched $^{13}CH_3OH$ (m/z = 33) was detected in the stoichiometric regime, but unlabeled $^{12}CH_3OH$ was observed in the steady state regime, thus suggesting that new, unlabeled ^{12}C methoxy species are formed after the initial ^{13}C methoxy species are hydrolyzed. Next, the reaction was allowed to proceed at steady state at a measured rate of 0.88 μmol

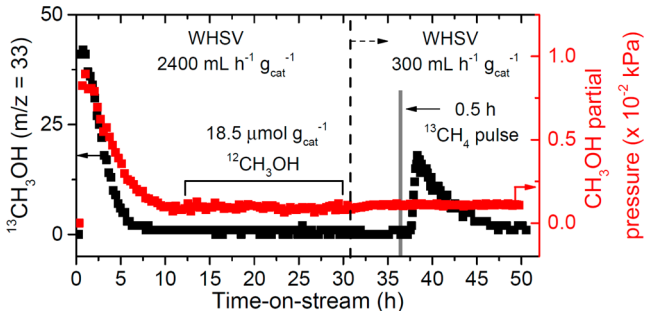

Figure 2. Transient, isotopically labeled kinetic experiments over Cu-Na-ZSM-5 (Cu/Al = 0.37, Na/Al = 0.26). Catalyst pretreatment: 5 h at 823 K under flowing O_2, cooled to 483 K under O_2 flow and purged under He for 0.5 h. Initial CH_4 oxidation: 0.5 h under 2400 mL h^{-1} g$_{cat}^{-1}$ of 17% $^{13}CH_4$/He at 483 K. Reaction conditions: T = 483 K, WHSV = 2400 mL h^{-1} g$_{cat}^{-1}$, P_{12CH_4} = 98.1 kPa, P_{H_2O} = 3.2 kPa, P_{O_2} = 0.0025 kPa (25 ppm). After 31 h on-stream, WHSV was reduced to 300 mL h^{-1} g$_{cat}^{-1}$ represented by the dashed line. Gray area denotes 0.5 h pulse of P_{13CH_4} = 98 kPa, P_{H_2O} = 3.2 kPa, P_{O_2} = 0.0025 kPa.

DOI: 10.1021/acscentsci.6b00139
ACS Cent. Sci. 2016, 2, 424−429

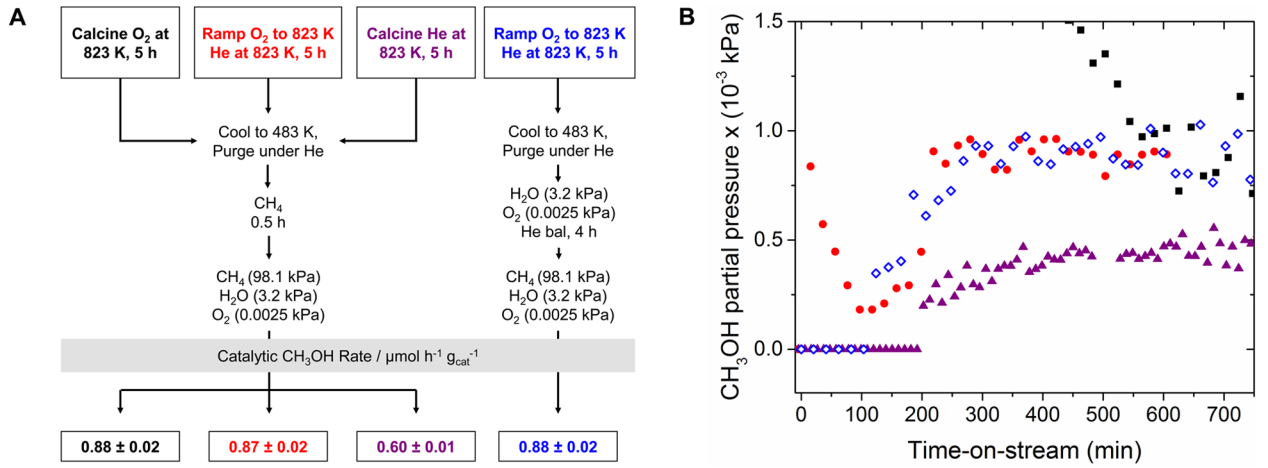

Figure 3. Thermal pretreatments and onset of steady state CH_4 oxidation over Cu-Na-ZSM-5 (Cu/Al = 0.37). (A) Thermal pretreatments, reaction conditions for all pretreatments, and catalytic CH_3OH production rates. The symbol ± denotes 95% confidence interval. (B) Evolution of catalytic CH_3OH production for each pretreatment outlined in (A); t = 0 denotes when the $CH_4/H_2O/O_2$ gas flow was started. Reaction conditions: T = 483 K, WHSV = 2400 mL h^{-1} g_{cat}^{-1}, PCH_4 = 98.1 kPa, P_{H_2O} = 3.2 kPa, P_{O_2} = 0.0025 kPa.

CH_3OH h^{-1} g_{cat}^{-1} for 21 h (equivalent to the production of 18.5 μmol g_{cat}^{-1} of $^{12}CH_3OH$). At this point, the weight hourly space velocity (WHSV) was reduced from 2400 mL h^{-1} g_{cat}^{-1} to 300 mL h^{-1} g_{cat}^{-1}, and the gas mixture was switched to $^{13}CH_4/H_2O/O_2$ for 0.5 h before resuming the flow of the regular, unlabeled gas mixture. This effective pulse of labeled $^{13}CH_4$ resulted in the production of labeled $^{13}CH_3OH$ as evidenced by a detectable pulse of the m/z = 33 signal without significantly altering steady state production of CH_3OH (Figure 2). Similar ^{13}C enrichment profiles were observed for CO_2 during both isotope switching experiments (Figure S7). Analogous behavior was observed for similar experiments carried out over Cu-H-ZSM-5 (Figure S8). Control experiments using $^{12}CH_4$ to populate the activated catalyst with unlabeled ^{12}C methoxy species did not generate a significant amount of $^{13}CH_3OH$ in the stoichiometric or steady state regimes (Figures S6B, S8B), thereby ruling out artifacts or potential effects arising from natural abundance $^{13}CH_4$ in the unlabeled gas stream. Kinetic measurements on Cu-Na-ZSM-5 at 483 K show first, half, and zero order dependencies with respect to CH_4, H_2O, and O_2, respectively (Supporting Information Section S7, Figure S9). Importantly, replacing CH_4 with CD_4 in the extracting gas during steady state operation at a WHSV of 240 mL h^{-1} g_{cat}^{-1} decreased the CH_3OH production rate from 0.090 to 0.055 μmol h^{-1} g_{cat}^{-1} (Figure S10). This change corresponds to a kinetic isotope effect (KIE) of 1.6 ± 0.1, thus indicating that C−H abstraction is a kinetically relevant step in the catalytic cycle. Taken together, the data from the transient $^{13}CH_4$ pulse experiments, the reaction rate order dependencies, and the kinetic isotope effect confirm catalytic turnover.

Gas pretreatments were varied to gain insight into the origin of catalytic and stoichiometric sites in Cu-Na-ZSM-5 (see Figures 3, S11−12). Specifically, Cu-Na-ZSM-5 samples were subjected to three pretreatments at 873 K prior to regular CH_4 oxidation and extraction at 483 K: (i) calcination under O_2 and then under He (20 ppm of O_2); (ii) calcination under He (20 ppm of O_2); or (iii) calcination under He without O_2 (<0.1 ppm, Figure S11). In all cases, stoichiometric CH_3OH production drastically diminished (98−100%), but catalytic CH_3OH production was only moderately affected (0−60%) (Figure 3). Treating activated Cu-Na-ZSM-5 with He above 723 K has been shown to eliminate the mono-(μ-oxo) dicupric cores for stoichiometric CH_4 oxidation.[14] The absence of the mono-(μ-oxo) dicupric sites during steady state methane oxidation was confirmed with UV−visible spectroscopic and online gas chromatographic measurements over Cu-Na-ZSM-5 (Cu/Al = 0.37) (Supporting Information Section S9, Figures S13−S15). Interestingly, van Bokhoven et al. observed a small fraction of H_2O-tolerant sites in copper-exchanged mordenite (Cu-MOR) that did not require high temperature reactivation for stoichiometric CH_4 oxidation experiments after exposure to H_2O.[21,22] However, in the present study, exposing Cu-Na-ZSM-5 to H_2O/O_2/He at 483 K prior to contacting it with CH_4 completely eliminated stoichiometric CH_3OH production but did not affect catalytic CH_3OH production. Note the onset of the catalytic regime was nearly identical for all samples (240 min on-stream) after exposure to $CH_4/H_2O/O_2$ irrespective of the pretreatment used. The similarity of catalytic rates and onset of CH_3OH production for all pretreated Cu-Na-ZSM-5 samples implies the catalytic sites are different from those responsible for stoichiometric CH_4 oxidation, and the catalytic sites are either generated or activated when copper species are exposed to CH_4, H_2O, and O_2 at reaction conditions rather than during the high temperature pretreatment.

An induction period preceding the onset of catalytic CH_4 oxidation suggests that copper speciation changes under reaction conditions. The CH_3OH production profile for a regular CH_4 oxidation and extraction experiment using Cu-Na-ZSM-5 pretreated at 823 K first with O_2 and then with He (20 ppm of O_2) shows that catalytic production began after 240 min on-stream despite H_2O breaking through the catalyst bed after 25 min (Figure S12). A comparable induction process was observed when Cu-Na-ZSM-5 was pretreated without O_2 and exposed to a CH_4/H_2O gas mixture at 483 K (Figure S11). In this case CH_3OH was detected only ca. 300 min after O_2 was introduced into the system. Hydrated copper species are known to weakly associate with the zeolite framework, becoming mobile and easily oxidized.[23] In copper-exchanged zeolites with the chabazite topology (Cu-SSZ-13), hydrated Cu^{2+} ions have been shown to migrate under flowing wet O_2/N_2 (and trace NO and NH_3) gas mixtures between 403−523 K during the

DOI: 10.1021/acscentsci.6b00139
ACS Cent. Sci. 2016, 2, 424−429

Table 1. Catalytic CH_4 Oxidation Rates for Various Zeolite Topologies[a]

material	framework	cage shape	cage size (Å)[26]	channel size (Å)[27]	Si/Al_{nom}[b]	Si/Al_{tot}[c]	Cu/Al_{tot}[d]	specific activity[e]	STY ($h^{-1} \times 10^{-3}$)[f]
H-ZSM-5	MFI			5.3 × 5.6 5.1 × 5.5	11.5	13.2	0.31	1.79 ± 0.02	5.2 ± 0.05
H-Beta	BEA			6.6 × 6.7 5.6 × 5.6	12.5	13.3	0.30	0.80 ± 0.01	2.4 ± 0.04
MCM-41	MCM-41			30	12	16.1	0.74	0.36 ± 0.02	0.6 ± 0.03
H-ZSM-5	MFI			5.3 × 5.6 5.1 × 5.5	11.5	13.9	0.13	0.84 ± 0.02	6.0 ± 0.17
H-mordenite	MOR			6.5 × 7 2.6 × 5.7	10	11.1	0.14	0.84 ± 0.01	4.6 ± 0.08
H-ferrierite	FER			4.2 × 5.4 3.5 × 4.8	10	10.6	0.12	0.44 ± 0.01	2.7 ± 0.04
Na-ZSM-5	MFI			5.3 × 5.6 5.1 × 5.5	11.5	13.6	0.37	0.88 ± 0.02	2.2 ± 0.04
Na-Y	FAU	spherical	9.6 × 9.6	7.4 × 7.4	5.1	4.6	0.45	0.30 ± 0.01	0.3 ± 0.01
Na-SAPO-34	CHA	ellipsoidal	9.4 × 9.4 × 12.7	3.8 × 3.8	0.3	0.6	0.02	0.84 ± 0.03	7.9 ± 0.29
Na-SSZ-13	CHA	ellipsoidal	9.4 × 9.4 × 12.7	3.8 × 3.8	15	13.8	0.50	3.12 ± 0.01	6.1 ± 0.03
CuO_x-MFI[g]	MFI			5.3 × 5.6 5.1 × 5.5	∞	∞	∞	0	0
CuO_x-BEA[g]	BEA			6.6 × 6.7 5.6 × 5.6	∞	∞	∞	0	0
H-ZSM-5[g]	MFI			5.3 × 5.6 5.1 × 5.5	11.5	12.9	0	0	0

[a]Catalyst pretreatment: 5 h at 823 K under flowing O_2, cooled to 483 K under O_2 flow and then purged under He for 0.5 h. Initial CH_4 oxidation: 0.5 h under 2400 mL h^{-1} g_{cat}^{-1} CH_4 at 483 K. Reaction conditions: T = 483 K, WHSV = 2400 mL h^{-1} g_{cat}^{-1}, P_{CH_4} = 98.1 kPa, P_{H_2O} = 3.2 kPa, P_{O_2} = 0.0025 kPa (25 ppm). [b]Si/Al_{nom} denotes the nominal silicon to aluminum ratio in the zeolite based on commercial figures or ratios of SiO_2 to Al_2O_3 in synthesis procedures. [c]Si/Al_{tot} denotes the ratio of silicon to aluminum atoms ratio within the zeolite calculated using data from inductively coupled plasma mass spectrometry (ICP-MS) measurements. [d]Cu/Al_{tot} denotes the ratio of copper to aluminum atoms within the zeolite calculated using ICP-MS. [e]Specific activity = μmol_{CH_3OH} h^{-1} g_{cat}^{-1}. [f]Site time yield (STY) defined as mol CH_3OH (mol Cu)$^{-1}$ h^{-1}. [g]T = 483 K, WHSV = 2400 mL h^{-1} g_{cat}^{-1}, P_{CH_4} = 93.1 kPa, P_{H_2O} = 3.2 kPa, P_{O_2} = 0.051 kPa. The ± symbol denotes 95% confidence intervals.

selective catalytic reduction (SCR) of NO_x[24] to form transient dimeric active sites.[25] The strong similarities between the reaction temperature and the gaseous atmosphere (H_2O/O_2)used during both the SCR of NO_x and the oxidation of CH_4 could imply that mobile, hydrated copper species also rearrange into active sites for catalytic CH_4 oxidation as they do for the SCR of NO_x.

Catalytic CH_4 oxidation was investigated as a function of the copper content and Brønsted acidity of the zeolite (see Table S1). A control experiment with H-ZSM-5 (Si/Al = 11.5) not subjected to copper exchange did not generate CH_3OH (Table 1), thereby confirming that trace transition metal impurities in the zeolite are not responsible for catalytic behavior. Higher Cu/Al ratios in Cu-Na-ZSM-5 and Cu-H-ZSM-5 increased the steady state specific activity (defined as μmol_{MeOH} h^{-1} g_{cat}^{-1}), but decreased the site-time yield (STY, defined as mol_{CH_3OH} mol_{Cu}^{-1} h^{-1}), suggesting that the number of active sites does not increase proportionally with the total amount of copper. The presence of Brønsted acid sites increased specific activity and STY for all samples with similar Cu/Al ratios. Indeed, different apparent activation energies (E_a^{app}) were observed between the sodium and proton forms of Cu-ZSM-5 (Table S1). Density functional theory calculations over Cu-ZSM-5 have shown that Brønsted acid sites change the energetics of the formation of mono-(μ-oxo) dicupric cores with NO.[28] While mono-(μ-oxo) dicupric cores are likely not present under reaction conditions for catalytic CH_4 oxidation, Brønsted acid sites could impart similar changes in the energetics of formation of the catalytic sites.

The catalytic rates and E_a^{app} values of CH_4 oxidation are heavily influenced by zeolite topology (see Table 1, Table S1). Cu-MOR, featuring 12-membered ring (MR) pores intersected by sinusoidal 8-MR pores, exhibited either comparable or lower activity at 483 K than that of Cu-H-ZSM-5 (Table S1). However, a significantly higher E_a^{app} of 149 kJ/mol resulted in higher CH_3OH rates at temperatures above 483 K when compared to those of Cu-H-ZSM-5 (Figure S16). These results suggest the site speciation and reaction environment within MOR may play a role in stabilizing kinetically relevant transition states. Other topologies, including ferrierite (FER), beta (BEA), Y (FAU), and caged-based SSZ-13 and SAPO-34 (CHA) also oxidize CH_4 into CH_3OH but with different rates than those of ZSM-5. Zeolites with large pores at high Cu/Al (0.30−0.50) including BEA (12-MR, 6.6 × 6.7 Å and 5.6 × 5.6 Å) and FAU (7.4 × 7.4 Å windows) showed 50% and 70% lower overall activity when compared to MFI. MCM-41, an amorphous aluminosilicate with large pores of 30 Å, had nearly an order of magnitude lower STY than ZSM-5, indicating that a crystalline, microporous structure with small pores is preferable for catalytic CH_4 oxidation. At low Cu/Al (0.12−0.14), Cu-H-ZSM-5 has the highest specific activity and STY (Table 1), while FER (intersecting 10-MR [4.2 × 5.4 Å] and 8-MR [3.5 × 4.8 Å]) was half as active as ZSM-5. While Cu-ZSM-5 had the highest specific activity and STY compared to the small-pore zeolites tested, the cage-based aluminoslicate SSZ-13 and the silicoaluminophosphate SAPO-34 with the CHA topology (8-MR windows of 3.8 × 3.8 Å, ellipsoidal cages of 9.4 × 9.4 × 12.7 Å) featured higher STY of 6.1 × 10^{-3} h^{-1} and 7.9 × 10^{-3} h^{-1}, respectively, than those in Cu-Na-ZSM-5 or Cu-H-ZSM-5

DOI: 10.1021/acscentsci.6b00139
ACS Cent. Sci. 2016, 2, 424−429

at similar Cu/Al ratios (Table 1). These studies indicate the catalytic sites or the kinetically relevant transition states are sensitive to the zeolite topology, with materials featuring small pores or cage-based structures showing enhanced performance when compared to those with large pores.

Taking advantage of the large E_a^{app} for Cu-Na-SSZ-13 (Cu/Al = 0.50, 100 ± 2.1 kJ mol^{-1}), the reaction temperature was systematically increased to achieve higher catalytic rates. The site-time yield increased from 2.2 × 10^{-3} to 31.6 × 10^{-3} mol_{CH_3OH} (mol Cu)$^{-1}$ h^{-1} when increasing the temperature from 463 to 533 K before a decrease in rates was observed (Figure S17). The large E_a^{app} coupled with the stable CH_3OH production over a wide range of temperature suggest that Cu-SSZ-13 zeolites could be further engineered to enhance further catalytic rates. In summary, copper-exchanged zeolites offer a broad and robust platform for the low temperature, catalytic oxidation of CH_4 into CH_3OH using O_2.

The nature of the catalytic active sites for CH_4 oxidation into CH_3OH over copper-exchanged zeolites is currently unknown. A recent report by von Bokhoven et al. observed the formation of copper oxide clusters in Cu-MOR after the cyclic, isothermal, and stoichiometric oxidation of CH_4 into CH_3OH.[22] It was hypothesized that these oxide clusters were active for isothermal cyclic CH_4 oxidation. We did not observe steady state activity for large copper oxide nanoparticles supported on pure silica MFI between 483 and 543 K (average size 30 nm for CuO_x, Table 1, Figures S18−20) or on pure silica BEA (average size 60 nm for Cu_2O, 41 nm for CuO, Table 1, Figures S21−22). However, we cannot rule out that ultrasmall copper oxide clusters, or copper species stabilized by aluminum in the zeolite framework or in defect sites are responsible for catalytic activity. Diffuse reflectance UV−visible spectroscopic measurements show peaks forming at 20 800, 26 800, and 30 000 cm^{-1} during steady state CH_3OH production (Figure S15C.1−2, D.1−2), possibly corresponding to copper oxide species[29] generated during reaction. Future work will focus on identifying and characterizing the catalytic site(s) as well as devising strategies to maximize catalytic activity.

■ ASSOCIATED CONTENT

Supporting Information

The Supporting Information is available free of charge on the ACS Publications website at DOI: 10.1021/acscentsci.6b00139.

Experimental details, product identification for catalytic CH_4 oxidation over Cu-Na-ZSM-5, simulation of high conversion CH_4 oxidation over Cu-Na-ZSM-5, control experiments for isotopically labeled kinetic experiments, kinetic order of reactants over Cu-Na-ZSM-5, thermal and gas pretreatments on Cu-Na-ZSM-5, in-situ UV−visible spectra of Cu-Na-ZSM-5, kinetic data of CH_4 oxidation over Cu-ZSM-5 and Cu-MOR, CH_4 oxidation vs temperature over Cu-Na-SSZ-13, powder X-ray diffraction patterns and CH_4 oxidation vs temperature over CuO_x on silica MFI and BEA, powder X-ray diffraction patterns of ZSM-5 and MOR, elemental composition, pore volume, and surface area of ZSM-5, MOR, and SSZ-13 (PDF)

■ AUTHOR INFORMATION

Corresponding Author

*E-mail: yroman@mit.edu.

Notes

The authors declare the following competing financial interest(s): The authors and MIT have filed a patent on the results presented herein.

■ ACKNOWLEDGMENTS

This work was supported by the Massachusetts Institute of Technology Energy Initiative's Seed Fund (K.N. and Y.R.L.) and the Japanese Government via Postdoctoral Fellowships for Research Abroad from the Japan Society for the Promotion of Science (K.I.). ^{1}H NMR spectra were collected at the Massachusetts Institute of Technology Department of Chemistry Instrumentation Facility (DCIF) supported by the National Science Foundation (Award Nos. CHE-9808061 and DBI-9729592).

■ REFERENCES

(1) Periana, R. A.; Taube, D. J.; Gamble, S.; Taube, H.; Satoh, T.; Fujii, H. Platinum catalysts for the high-yield oxidation of methane to a methanol derivative. *Science* **1998**, *280*, 560−564.

(2) Palkovits, R.; Antonietti, M.; Kuhn, P.; Thomas, A.; Schüth, F. Solid Catalysts for the Selective Low-Temperature Oxidation of Methane to Methanol. *Angew. Chem., Int. Ed.* **2009**, *48*, 6909−6912.

(3) Smith, K. T.; Berritt, S.; González-Moreiras, M.; Ahn, S.; Smith, M. R.; Baik, M.-H.; Mindiola, D. J. Catalytic borylation of methane. *Science* **2016**, *351*, 1424−1427.

(4) Caballero, A.; Despagnet-Ayoub, E.; Mar Díaz-Requejo, M. M.; Díaz-Rodríguez, A.; González-Núñez, M. E.; Mello, R.; Muñoz, B. K.; Ojo, W.-S.; Asensio, G.; Etienne, M.; Perez, P. J. Silver-Catalyzed CC Bond Formation Between Methane and Ethyl Diazoacetate in Supercritical CO_2. *Science* **2011**, *332*, 835−838.

(5) Cavaliere, V. N.; Mindiola, D. J. Methane: a new frontier in organometallic chemistry. *Chem. Sci.* **2012**, *3*, 3356−3365.

(6) Lieberman, R. L.; Rosenzweig, A. C. Crystal structure of a membrane-bound metalloenzyme that catalyses the biological oxidation of methane. *Nature* **2005**, *434*, 177−182.

(7) Balasubramanian, R.; Smith, S. M.; Rawat, S.; Yatsunyk, L. A.; Stemmler, T. L.; Rosenzweig, A. C. Oxidation of methane by a biological dicopper centre. *Nature* **2010**, *465*, 115−119.

(8) Shu, L.; Nesheim, J. C.; Kauffmann, K.; Münck, E.; Lipscomb, J. D.; Que, L. An Fe2IVO2 diamond core structure for the key intermediate Q of methane monooxygenase. *Science* **1997**, *275*, 515−518.

(9) Panov, G.; Sobolev, V.; Dubkov, K.; Parmon, V.; Ovanesyan, N.; Shilov, A.; Shteinman, A. Iron complexes in zeolites as a new model of methane monooxygenase. *React. Kinet. Catal. Lett.* **1997**, *61*, 251−258.

(10) Ovanesyan, N.; Shteinman, A.; Dubkov, K.; Sobolev, V.; Panov, G. The state of iron in the Fe-ZSM-5-N2O system for selective oxidation of methane to methanol from data of Mössbauer spectroscopy. *Kinet. Catal.* **1998**, *39*, 792−797.

(11) Groothaert, M. H.; Smeets, P. J.; Sels, B. F.; Jacobs, P. A.; Schoonheydt, R. A. Selective oxidation of methane by the bis (μ-oxo) dicopper core stabilized on ZSM-5 and mordenite zeolites. *J. Am. Chem. Soc.* **2005**, *127*, 1394−1395.

(12) Narsimhan, K.; Michaelis, V. K.; Mathies, G.; Gunther, W. R.; Griffin, R. G.; Román-Leshkov, Y. Methane to acetic acid over Cu-exchanged zeolites: mechanistic insights from a site-specific carbonylation reaction. *J. Am. Chem. Soc.* **2015**, *137*, 1825−1832.

(13) Woertink, J. S.; Smeets, P. J.; Groothaert, M. H.; Vance, M. A.; Sels, B. F.; Schoonheydt, R. A.; Solomon, E. I. A [Cu2O] 2+ core in Cu-ZSM-5, the active site in the oxidation of methane to methanol. *Proc. Natl. Acad. Sci. U. S. A.* **2009**, *106*, 18908−18913.

(14) Smeets, P. J.; Groothaert, M. H.; Schoonheydt, R. A. Cu based zeolites: A UV−vis study of the active site in the selective methane oxidation at low temperatures. *Catal. Today* **2005**, *110*, 303−309.

DOI: 10.1021/acscentsci.6b00139
ACS Cent. Sci. 2016, 2, 424−429

(15) Alayon, E. M.; Nachtegaal, M.; Ranocchiari, M.; van Bokhoven, J. A. Catalytic conversion of methane to methanol over Cu–mordenite. *Chem. Commun.* **2012**, *48*, 404–406.
(16) Hammond, C.; Forde, M. M.; Ab Rahim, M. H.; Thetford, A.; He, Q.; Jenkins, R. L.; Dimitratos, N.; Lopez-Sanchez, J. A.; Dummer, N. F.; Murphy, D. M.; Carley, A. F.; Taylor, S. H.; Willock, D. J.; Stangland, E. E.; Kang, J.; Hagen, H.; Kiely, C. J.; Hutchings, G. J. Direct Catalytic Conversion of Methane to Methanol in an Aqueous Medium by using Copper-Promoted Fe-ZSM-5. *Angew. Chem., Int. Ed.* **2012**, *51*, 5129–5133.
(17) Vanelderen, P.; Snyder, B. E.; Tsai, M.-L.; Hadt, R. G.; Vancauwenbergh, J.; Coussens, O.; Schoonheydt, R. A.; Sels, B. F.; Solomon, E. I. Spectroscopic definition of the copper active sites in Mordenite: selective methane oxidation. *J. Am. Chem. Soc.* **2015**, *137*, 6383–6392.
(18) Grundner, S.; Markovits, M. A.; Li, G.; Tromp, M.; Pidko, E. A.; Hensen, E. J.; Jentys, A.; Sanchez-Sanchez, M.; Lercher, J. A. Single-site trinuclear copper oxygen clusters in mordenite for selective conversion of methane to methanol. *Nat. Commun.* **2015**, *6*, 7546.
(19) Grundner, S.; Luo, W.; Sanchez-Sanchez, M.; Lercher, J. A. Synthesis of single-site copper catalysts for methane partial oxidation. *Chem. Commun.* **2016**, *52*, 2553–2556.
(20) Wulfers, M. J.; Teketel, S.; Ipek, B.; Lobo, R. Conversion of methane to methanol on copper-containing small-pore zeolites and zeotypes. *Chem. Commun.* **2015**, *51*, 4447–4450.
(21) Alayon, E. M. C.; Nachtegaal, M.; Bodi, A.; van Bokhoven, J. A. Reaction Conditions of Methane-to-Methanol Conversion Affect the Structure of Active Copper Sites. *ACS Catal.* **2014**, *4*, 16–22.
(22) Tomkins, P.; Mansouri, A.; Bozbag, S. E.; Krumeich, F.; Park, M. B.; Alayon, E. M. C.; Ranocchiari, M.; van Bokhoven, J. A. Isothermal Cyclic Conversion of Methane into Methanol over Copper-Exchanged Zeolite at Low Temperature. *Angew. Chem.* **2016**, *128*, 5557–5561.
(23) Palomino, G. T.; Fisicaro, P.; Bordiga, S.; Zecchina, A.; Giamello, E.; Lamberti, C. Oxidation states of copper ions in ZSM-5 zeolites. A multitechnique investigation. *J. Phys. Chem. B* **2000**, *104*, 4064–4073.
(24) Gao, F.; Kwak, J. H.; Szanyi, J.; Peden, C. H. Current understanding of cu-exchanged Chabazite molecular sieves for use as commercial diesel engine DeNOx catalysts. *Top. Catal.* **2013**, *56*, 1441–1459.
(25) Gao, F.; Walter, E. D.; Kollar, M.; Wang, Y.; Szanyi, J.; Peden, C. H. F. Understanding ammonia selective catalytic reduction kinetics over Cu/SSZ-13 from motion of the Cu ions. *J. Catal.* **2014**, *319*, 1–14.
(26) Chen, J.; Li, J.; Wei, Y.; Yuan, C.; Li, B.; Xu, S.; Zhou, Y.; Wang, J.; Zhang, M.; Liu, Z. Spatial confinement effects of cage-type SAPO molecular sieves on product distribution and coke formation in methanol-to-olefin reaction. *Catal. Commun.* **2014**, *46*, 36–40.
(27) Baerlocher, C.; McCusker, L. B. *Database of Zeolite Structures*, http://www.iza-structure.org/databases/.
(28) Sajith, P. K.; Shiota, Y.; Yoshizawa, K. Role of Acidic Proton in the Decomposition of NO over Dimeric Cu(I) Active Sites in Cu-ZSM-5 Catalyst: A QM/MM Study. *ACS Catal.* **2014**, *4*, 2075–2085.
(29) Vanelderen, P.; Hadt, R. G.; Smeets, P. J.; Solomon, E. I.; Schoonheydt, R. A.; Sels, B. F. Cu-ZSM-5: A biomimetic inorganic model for methane oxidation. *J. Catal.* **2011**, *284*, 157–164.

DOI: 10.1021/acscentsci.6b00139
ACS Cent. Sci. 2016, 2, 424–429